https://doi.org/10.5194/acp-2022-641
Preprint. Discussion started: 4 October 2022

Atmospheric Chemistry and Physics Discussions

Distribution of cross-tropopause convection within the Asian monsoon region from May through October 2017

Corey E. Clapp[1], Jessica B. Smith[1], Kristopher M. Bedka[2], James G. Anderson[1,3,4]

[1]Harvard John A. Paulson School of Engineering and Applied Sciences, Harvard University, Cambridge, 02138, U.S.A.
[2]NASA Langley Research Center, Hampton, 23681, U.S.A.
[3]Department of Chemistry and Chemical Biology, Harvard University, Cambridge, 02138, U.S.A.
[4]Department of Earth and Planetary Sciences, Harvard University, Cambridge, 02138, U.S.A.

Correspondence to: Corey E. Clapp (cclapp@fas.harvard.edu)

Abstract. We constructed a database of cross-tropopause convection in the Asian monsoon region for the months of May through October of 2017 using overshooting tops (OTs), deep convective features that penetrate the local cirrus anvil layer and the local tropopause, with Meteosat-8 geostationary satellite detections. The database of 40,918 OTs, represents a hemispheric record of convection covering the study domain from 10°S to 55°N and from 40 to 115°E. With this database, we analyzed the geographic, monthly, and altitude distribution of this convection and compared it to the convective distributions represented by satellite observations of outgoing longwave radiation (OLR) and precipitation. We find that cross-tropopause convection is most active during the months of May through August (with daily averages of these months above 300 OTs/day) and declines through September and October. Most of this convection occurs within North and South India, the Bay of Bengal, and the Indian Ocean regions, which together account for 75.1% of all OTs. We further identify distinct, differing seasonal trends within the study subregions. For the North India, South India, and Bay of Bengal regions the distribution of OTs follows the development of the Asian Monsoon, with its north-south movement across the study period. This work demonstrates that when evaluating the effects of convection on lower stratospheric composition over the Asian monsoon region it is important to both consider cross-tropopause convection and the contributions across the entire region due to the significant geographic and monthly variation in convective activity.

1 Introduction

Deep convection in the Asian monsoon region provides an important pathway for the transport of boundary layer air to the stratosphere. Which areas within the Asian monsoon region, however, contribute the most to this convective transport remain uncertain. Moreover, while the current understanding of convective transport considers deep convection that reaches the upper troposphere, less attention has been paid to the role of cross-tropopause convection (Legras & Bucci, 2020; Tissier & Legras, 2016). To investigate the potential impacts of cross-tropopause convection on convective transport and the composition of the lower stratosphere we construct a seasonal database of "overshooting tops," (OTs) deep convective

https://doi.org/10.5194/acp-2022-641
Preprint. Discussion started: 4 October 2022

Atmospheric Chemistry and Physics Discussions

updrafts that penetrate both the cirrus anvil layer and the local tropopause, in the Asian monsoon region from geostationary satellite infrared imagery for the period of May through October of 2017. With this database we identify the primary source regions of cross-tropopause convection as well as the seasonal and altitude trends of this deep convection. Understanding the convective transport within the Asian monsoon is critical to understanding the transport of both radiatively and chemically active species from the boundary layer to the lower stratosphere. In particular, assessing the timing and location of convection is necessary to predict which species in what quantities from the source region boundary layer are transported as well as their impacts on the lower stratosphere.

The Asian monsoon is associated with significant convectively sourced contributions to the composition of the lower stratosphere. Observations of this convective influence range from large-scale satellite studies to small scale in situ measurements. Satellite observations have shown consistent indications of tropospheric influence in water vapor and carbon monoxide maxima as well as ozone minima concurrent with the Asian monsoon anticyclone that develops in the UTLS region (Luo et al., 2018; Park et al., 2007; Randel et al., 2010; Santee et al., 2017). Modelling studies, including chemistry-climate models (e.g. Pan et al., 2016; Wu et al., 2020) and Lagrangian-trajectory models (e.g. Legras & Bucci, 2020; Tissier & Legras, 2016), have corroborated the convective source of these perturbations. Further, recent in situ measurements have also verified their convective origins (Bucci et al., 2020; Johansson et al., 2020; von Hobe et al., 2021).

The convective transport of boundary layer air to the UTLS over the Asian monsoon impacts the concentrations of many chemical species that are both radiatively and chemically significant. Beyond the water vapor, carbon monoxide, and ozone observations mentioned previously, deep convection has been shown to transport anthropogenic pollutants such as peroxyacetyl nitrate and acetylene (Johansson et al., 2020), and other non-methane hydrocarbons (Baker et al., 2011). Both satellite and in situ measurements have also indicated that deep convection is the primary source of the aerosols in the UTLS in the Asian monsoon region (Vernier et al., 2015; Vernier et al., 2018). Furthermore, this convection may transport very-short lived species (VSLS), including ozone depleting substances (ODS), to the UTLS (Fiehn et al., 2018; Hossaini et al., 2016; Tegtmeier et al., 2020).

Moreover, the impact of the transport of tropospheric air and pollutants into the lower stratosphere is not confined to the AMA. Both eastward and westward eddy shedding by the AMA has the potential to transport pollutants and boundary layer air from the Asian monsoon region into the midlatitudes and global stratosphere (Fadnavis et al., 2018; Garny & Randel, 2013; Popovic & Plumb, 2001; Vogel et al., 2014). In situ measurements of stratospheric air with perturbed chemical compositions sourced back to the AMA have been observed in the midlatitudes of the Northern Hemisphere (Lelieveld et al., 2018; Muller et al., 2016; Rolf et al., 2018).

The location and timing of the initial deep convection influence both the chemical impact of convective transport on the composition of the UTLS and the geographic distribution of that impact. Due to the heterogeneity of surface emissions within the Asian monsoon region, the chemical composition of convectively transported boundary layer air will vary significantly depending on the source region. Furthermore, the location of the initial convective transport determines the pathway of entry into the lower stratosphere and therefore which regions are impacted “downstream” in the large-scale

https://doi.org/10.5194/acp-2022-641
Preprint. Discussion started: 4 October 2022


Atmospheric Chemistry and Physics Discussions

circulation. For example, several studies investigating the ozone depleting potentials (ODPs) of various chemical species have found that the influence of source regions and seasons alone results in significantly different ODPs for the same emissions (Brioude et al., 2010; Claxton et al., 2019; Pisso et al., 2010; Tegtmeier et al., 2020). Therefore, understanding the distribution of deep convection within the Asian monsoon region is necessary to predict its net effect on the composition of the UTLS, both locally and globally.

Prior work on convective influence within the Asian monsoon region has focused primarily on convective transport from the boundary layer to upper troposphere followed by diabatic heating and ascent pathway to the lower stratosphere. Yet, the relative importance of various source regions remains unclear. For example, some studies have found that deep convection over the Tibetan Plateau is a key contributor (Bergman et al., 2013; Fu et al., 2006; Heath & Fuelberg, 2014; Pan et al., 2016; Wu et al., 2020), while others have identified the Bay of Bengal and the west Pacific as critical source regions (Chen et al., 2012; Devasthale & Fueglistaler, 2010; James et al., 2008). Other studies have suggested that while the Tibetan Plateau may present a uniquely efficient pathway into the UTLS, it is a minority contributor compared to other source regions including the Asian mainland (Legras & Bucci, 2020; Tissier & Legras., 2016). Moreover, these convective source regions are found to have distinct tropopause-crossing regions (Chen et al., 2012). Much of this uncertainty likely arises from the difficulty in accounting for, or resolving, the small temporal and spatial-scales necessary to represent convection.

Previous studies investigating the global distribution and frequency of extreme convection using non-Sun-synchronous satellite observations have shown the Asian monsoon region to be of importance (Liu & Liu, 2016; Liu et al., 2020; Zipser et al., 2006). This work also found that extreme convection was more likely to occur over land than over ocean, and that the mid-latitudes contributed equally to the tropics. Importantly, when considering extreme convection that reached or surpassed the tropopause, the Asian monsoon region remained an area of significant activity (Liu & Liu, 2016; Liu et al., 2020).

The present analysis builds on prior studies of the convective transport of boundary layer air into the lower stratosphere and of the frequency of intense convection over the Asian monsoon region, and focuses specifically on cross-tropopause convection exploiting convective features (OTs), which represent both the finest-scale and deepest convection, to assess convective transport directly into the lower stratosphere within this specific region. Using OTs identified with geostationary satellite infrared imagery (Bedka & Khoplenkov, 2016), we construct a database of cross-tropopause convection, and describe the geographic, monthly and altitude distribution of this convection over the Asian monsoon region from May through October of 2017. We also compare this distribution of cross-tropopause convection to the distribution of overall convection as represented by satellite observations of outgoing longwave radiation (OLR) and precipitation for the same period and region. This work is complementary to the previously discussed studies which focused on tropospheric convection that reaches altitudes above the level of zero radiative heating before slowly ascending into the stratosphere diabatic heating. Here, we assess the potential impact of extreme convection that directly reaches the lower stratosphere, a transport mechanism which bypasses slow-ascent across the tropopause.

https://doi.org/10.5194/acp-2022-641
Preprint. Discussion started: 4 October 2022


Atmospheric Chemistry and Physics Discussions

2 Data and Methods

2.1 OT database

The OT database, derived from Meteosat-8 data, represents a hemispheric record of convection covering the study domain from 10°S to 55°N and from 40 to 115°E for the time period of 01 May, 2017 through 31 October, 2017. The OTs are algorithmically identified using multispectral imagery from Meteosat-8 with a horizontal resolution of approximately 4 km (Bedka & Khlopenkov, 2016; Yost et al., 2018). Updrafts that overshoot their anvil altitude but do not reach the tropopause are not included in this study. Only OTs with detection probability ratings (as determined by the temperature differences between the OT and the anvil, tropopause as identified with the WMO lapse-rate definition and the MERRA-2 reanalysis data, and local level of neutral buoyancy) greater than or equal to 0.9 were used in this analysis. This threshold detected ~50% of human-identified OTs randomly sampled throughout the world (Bedka & Khlopenkov, 2016). At this rating, the false detection rate was determined to be ~10%, and these errant detections were typically found in close proximity to actual OT regions, so inclusion of these samples does not adversely affect the results. The Bedka and Khlopenkov (2016) OT identification method is a conservative methodology that underpredicts OTs allowing for high confidence in the OTs that are detected. The potential temperature of each OT was derived from the OT IR temperature and pressure derived from the OT height and MERRA-2 (Gelaro et al., 2017) reanalysis, using the method of Griffin et al. (2016).

The OT database does not represent a complete budget of cross-tropopause convection occurring in the study region and over the time period considered. This is because the Meteosat-8 OT data were acquired every 15 minutes, while the average lifetime of an OT can be as short as several minutes (Bedka & Khlopenkov, 2016). Consequently, the OT dataset used in this study represents a small percentage of the total number of OTs that occurred and should not be used to estimate total convective outflow. The OT database, however, is still valid for analyzing large scale trends and distributions because the consistent and frequent sampling, the long time period under study, and the large region of interest retain the major features of OT frequency, depth, and geographic distribution. This OT detection methodology has been used in prior studies of the geographic and seasonal distributions of cross-tropopause convection (Clapp et al., 2019; Clapp et al., 2021).

2.2 Study regions

To identify regional differences in geographic, monthly, and vertical distribution of OTs, the study domain was subdivided into 12 regions. These regions (see Figure 1c) were selected to capture geographically distinct areas of cross-tropopause convection and to allow for comparison to prior work that has examined sources of convective influence on the lower stratosphere in the Asian monsoon region. Further, many of these regions have been shown to have differences in convective characteristics such as convective initiation mechanisms and seasonal dependences (Romatschke & Houze, 2011).

https://doi.org/10.5194/acp-2022-641
Preprint. Discussion started: 4 October 2022


Atmospheric Chemistry and Physics Discussions

The Tibetan Plateau region was included because prior studies have identified it as a significant source region of convective influence on the UTLS, and has a unique convective environment due to its topography as well as its central location within the Asian monsoon anticyclone (e.g. Bergman et al., 2013; Heath & Fuelberg, 2014). The southern edge of the region, between 70° E and 95° E, which separates it from the North India region, is defined by the 3 km topographic height, taken from the MERRA-2 reanalysis. Similar boundaries have been used previously (e.g. Fu et al., 2006; Heath & Fuelberg, 2014).

The North and South India regions were included to capture the primary areas of land-based Asian monsoon convection. The separate regions are necessary to distinguish the differences in seasonality, such as monsoon onset (Kajikawa et al., 2012; Walker & Bordoni, 2016), and convective character, such as the importance of orography to convective initiation in North India (Romatschke & Houze, 2011). This distinction has also been used in prior work (e.g. Fu et al., 2006; Heath & Fuelberg, 2014). The Bay of Bengal, Arabian Sea, and Indian Ocean regions were defined to account for oceanic monsoon convection. The Indian Ocean region captures and separates the influence of the ITCZ, seen in the OT distribution (Figure 1a), from the other two regions. The Bay of Bengal region has also been previously studied as a region of significant convective influence (e.g. Devasthale et al., 2010)

The Southeast Asia, East China, and West Pacific regions were included to distinguish the eastern portion of the Asian monsoon from the subcontinental convection, which is expected to have different seasonal trends and large-scale drivers (Wang et al., 2001; Wei et al., 2015; Yihui & Chan, 2005).The Arabian Peninsula region was included to investigate the climatology of the high density of OTs observed over the southwest Arabian Peninsula and Ethiopia (Figure 1a). The remaining areas within the study region, in which few OTs are observed, are covered by the Northern Latitudes, and Africa regions.

2.3 OLR and precipitation data

The OLR data is taken from the NOAA Interpolated Outgoing Longwave Radiation climatology, which has a global coverage and a resolution of 2.5° x 2.5° (Liebmann & Smith, 1996). The precipitation data is from the Global Precipitation Climatology Project (GPCP) Climate Data Record (CDR), which has global coverage and a resolution of 1° x 1° (Huffman et al., 2001).

3 Results

We begin with an analysis of the geographic distribution of all OTs observed across the entire study region and time period. We then compare the distribution of cross-tropopause convection with other convective indicators: OLR as a proxy for deep convection, and daily precipitation as an indicator of general tropospheric convection. The results of this analysis are then used to identify specific regions of interest for cross-tropopause convection within the larger context of monsoon convection.

https://doi.org/10.5194/acp-2022-641
Preprint. Discussion started: 4 October 2022

Atmospheric Chemistry and Physics Discussions

3.1 Geographic and seasonal distribution of cross-tropopause convection

Figure 1a shows the geographic locations of all OTs across the study region for the entire study period, May through October of 2017. OTs are binned into a latitude-longitude grid of 1°x1° resolution. Areas of significant cross-tropopause convection include northern India (in particular the northwestern coast, and north coast of the Bay of Bengal), and the Bay of Bengal. The Indian Ocean shows a high volume of dispersed cross-tropopause convection located at the ITCZ in an east-west band between 0-5° N. In contrast, the southern edge of the Arabian Peninsula has a smaller number of OTs that are highly concentrated enough to show number densities comparable to the largest source regions (174 in the Arabian Peninsula region compared to 154 and 183 in the North India and Bay of Bengal regions, respectively). This high count of intense convective events has been previously observed (Liu & Liu, 2016; Liu et al., 2020; Zipser et al., 2006). The distribution shows the importance of both land-based and oceanic convection with significant quantities of cross-tropopause convection occurring in both environments.

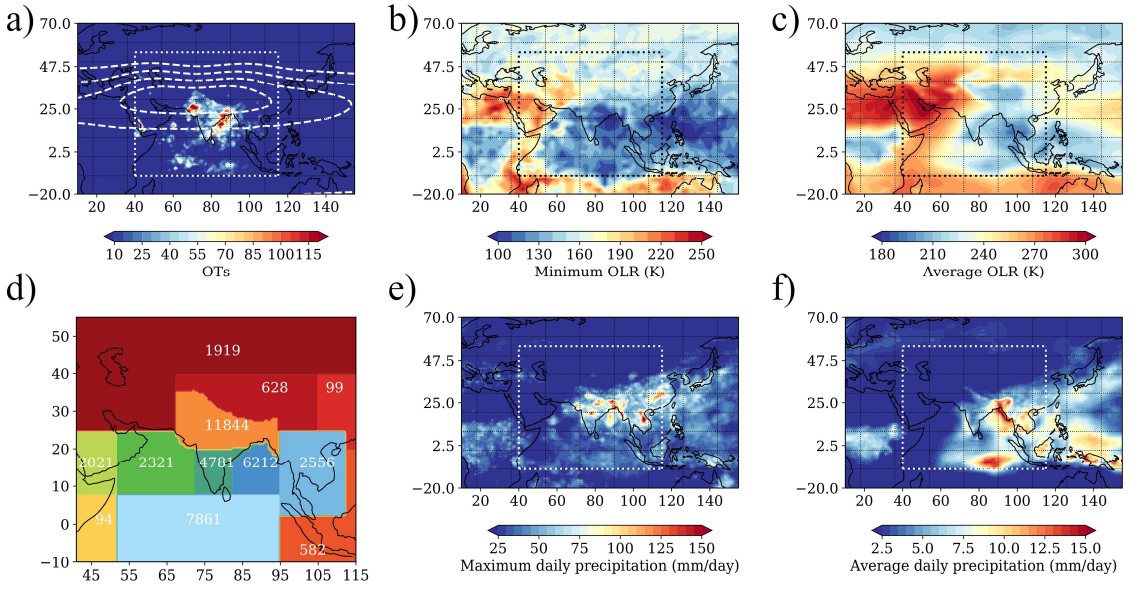

Figure 1 The geographic distribution of convection over the Asian monsoon region during the study period (May 1, 2017 through October 31, 2017). Cross-tropopause convection is shown in Figure 1a, which depicts the distribution of OTs, binned by 1° x 1°, within the satellite observation window (dotted-white box) and with the average Montgomery potential stream-function at 400 K for the months of JJA (dashed white contours from $3.59x10^5$ m^2s^{-2} to $3.63x10^5$ m^2s^{-2} by $0.01x10^5$ m^2s^{-2}) to illustrate the location of the Asian monsoon anticyclone. Figure 1d shows the boundaries of the areas used for the regional analysis as well as the total OTs observed in each region. The minimum and average daily OLR values are shown in Figures 1b and 1c, respectively. The minimum and average daily precipitation are shown in Figures 1e and 1f, respectively.

https://doi.org/10.5194/acp-2022-641
Preprint. Discussion started: 4 October 2022


Atmospheric Chemistry and Physics Discussions

Another significant feature is the lack of cross-tropopause convection occurring over the Tibetan Plateau. A large quantity of OTs is observed over the southern slope of the plateau, however, this topography corresponds to a distinct boundary north of which few OTs occur. This is consistent with the conclusions of Tissier and Legras (2016) and Legras and Bucci (2020) in which the Tibetan Plateau is not a numerically significant contributor to convective transport, but is particularly efficient due to the central location within the AMA. Here, convection over the Tibetan Plateau detrains boundary layer air in the upper troposphere, but the subsequent diabatic ascent into the lower stratosphere occurs primarily in neighboring regions. Similarly, the distributions observed in the global studies of extreme convection also exhibit a ridge of increased frequency along the southern slope but few convective events over the Tibetan Plateau itself (Liu & Liu, 2016; Liu et al., 2020; Zipser et al., 2006). Further, Devasthale and Fueglistaler (2010) find that while there is a significant cloud fraction over the Tibetan Plateau during July and August at 200 and 150 hPa, at 100 hPa there is almost none. Our climatology of cross-tropopause convection confirms that convection rarely directly transports boundary layer air into the lower stratosphere over the Tibetan Plateau.

Figures 1b and 1c show the OLR minimum and average daily value for the entire study period. The minimum OLR spatial trends, as a proxy for the "deepest" convection, recreate the cross-tropopause convective distribution better than the average. In particular, north India, the Bay of Bengal and the Indian Ocean are regions of significant convective activity. The convective activity over the Arabian Peninsula visible in the OT distribution, however, is not shown to the same degree in the OLR data. The greatest disagreement with the OT distribution is present in the average daily OLR over the Tibetan Plateau, which has values comparable to the other major convective regions. This is likely a consequence of the unique atmospheric structure resulting from the high altitude of the region resulting in particularly low OLR values for tropospheric convection. This could also be a consequence of frequent convection within the Tibetan Plateau region that is, however, not as intense as the regions marked by high OT counts.

Figures 1c and 1d show the GPCP maximum daily precipitation and average daily precipitation for the entire study period. When comparing the geographic distribution of cross-tropopause convection to the distribution of precipitation, there is significant agreement. The Bay of Bengal and northern India remain dominant regions of convection, and the spatial distribution within these regions are also similar with the largest values in the northern Bay, immediately north of the Bay, and in the northwest of India. Further, the southern slope also forms a ridge of high precipitation values, northward of which there is less activity. The large maximum precipitation values in central India, however, do not correspond with an OT activity. The Indian Ocean also shows a band of precipitation at the ITCZ, similar to the band of cross-tropopause convection, although of lesser magnitude. The high concentration of convective activity visible in the OT distribution over the Arabian Peninsula, however, is not present in the precipitation data. This is a potential consequence of the convective events over the Arabian Peninsula being small, and therefore not detected by the relatively coarse GPCP and OLR observations. Similarly, there is a large concentration of high precipitation over southeast Asia which is not reflected in the OT observations, which could reflect convection characterized by high moisture, but few OTs.

https://doi.org/10.5194/acp-2022-641
Preprint. Discussion started: 4 October 2022

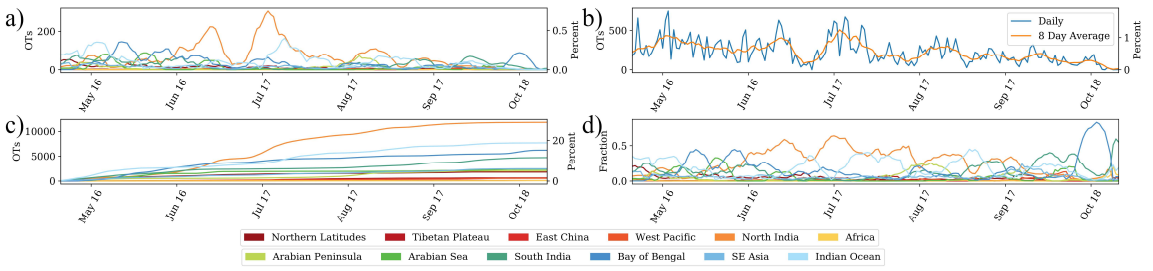

Figure 2 The seasonal development of cross-tropopause convection within the study region. Figure 1a shows the time series of the daily absolute number (left axis) and percent (right axis) of OTs observed within each region, as indicated by color. Figure 1b shows the time series of the total daily number (left axis) and percent (right axis) of OTs in blue as well as the rolling 8 day average in orange. Figure 1c shows the cumulative total number (left axis) and percent (right axis) of OTs within each region, as indicated by color, as a function of time. Figure 1d shows the daily-normalized fractional contribution of each region, as indicated by color, as a function of time.

Figure 2 displays the seasonal development of cross-tropopause convection. As seen in Figure 2b, during the active period of May through August, the daily number of OTs fluctuates largely between 200-400 OTs per day. As the monsoon season declines through September and October so does the frequency of cross-tropopause convection. For example, the active months of May through August contribute on average 22.9% of the total OTs while September and October contribute 13.4% and 6.3%, respectively. From Figure 2a, however, it is clear that different regions dominate cross-tropopause convection at different times. For example, the North India region is the most important source region during June and July, while the Bay of Bengal and Indian Ocean regions are more significant in May.

Despite different source regions having time periods of particular significance, the North India region has the highest daily number of OTs observed (see the late June and early July peaks in Figure 2a). This indicates that although June and July have similar total amounts of cross-tropopause convection to May, these months are uniquely dominated by a single source region. This is emphasized in Figure 2d, in which during June and July, the largest daily fractional contribution values are visible for North India (0.59 on June 25th and 0.64 on July 14th). This daily fractional contribution is only surpassed in October by the Bay of Bengal region. This is an outlier, however, because there are much fewer total cross-tropopause events during this period, and this peak is likely caused by a specific event, a tropical depression within the Bay of Bengal.

From Figure 2c, the total impact of each region is visualized across these varying time periods of relative importance. North India has the greatest total amount of cross-tropopause convection (11,844 OTs, 29.0%). The Indian Ocean and Bay of Bengal regions are the next most significant contributors with 7861 OTs (19.2%) and 6212 OTs (15.2%) respectively, followed by the South India region with 4781 OTs (11.7%). Together the four largest contributors account for 75.1% of all OTs in the study area. Of the remaining OTs within the study area most are within the Southeast Asia region (2556 OTs, 6.3%), the Arabian Sea region (2321 OTs, 5.7%), and the Arabian Peninsula region (2021 OTs, 4.9%). The Northern Latitudes region has 1919 OTs (4.7%), however, given the large size of the region this is geographically dispersed. The Tibetan Plateau and the West Pacific regions have little cross-tropopause convection with 628 OTs (1.5%) and 582 OTs

https://doi.org/10.5194/acp-2022-641
Preprint. Discussion started: 4 October 2022

Atmospheric Chemistry and Physics Discussions

(1.4%) respectively. The remaining regions of East China and Africa have 99 OTs and 94 OTs respectively, less than 1.0% combined.

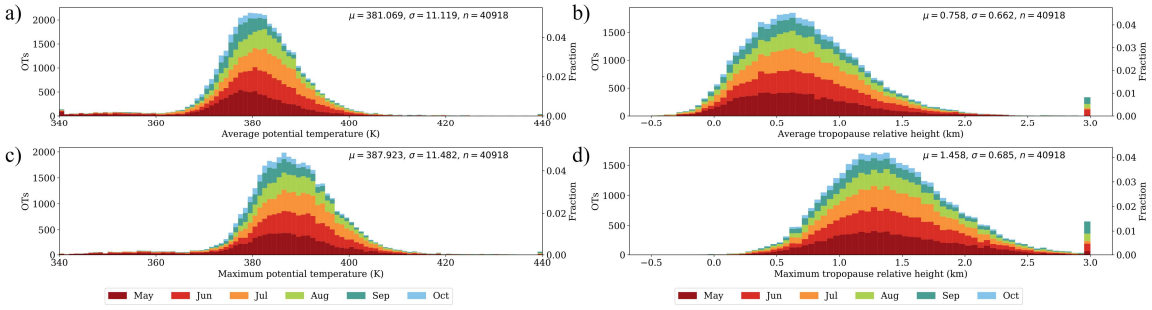

Figure 3 The altitude distribution of all OTs within the study region. Figures 1a and 1c show the distributions of the average and maximum potential temperature of each OT binned by 1 K, respectively. Figures 1b and 1c show the distributions of the average and maximum tropopause relative height of each OT binned by 0.05 km, respectively. Within each bin, color indicates the fractional contribution of each month. For example, the 1.25 km maximum tropopause relative height bin is comprised of 411 May OTs, 396 June OTs, 354 July OTs, 267 August OTs, 192 September OTs, and 93 October OTs. The mean, standard deviation, and number of OTs for each distribution is indicated in the upper-right corner.

Figure 3 shows frequency distributions for both the average and maximum potential temperature of OTs (Figures 3a and 3c) and the average and maximum altitude (Figures 3b and 3d) expressed in tropopause-relative coordinates over the study region for the entire study period. The color subdivisions indicate the proportions of cross-tropopause convection occurring during each month within each bin. For example, the 1.25 km maximum tropopause relative height bin is comprised of 411 May OTs, 396 June OTs, 354 July OTs, 267 August OTs, 192 September OTs, and 93 October OTs. Figures 3a and 3b show the average potential temperature and tropopause relative height, respectively, of the pixels within each OT. Figures 3c and 3d show the maximum potential temperature and tropopause relative height, respectively, of the pixels within each OT. As not all pixels of a given OT cross the tropopause, a small population of OTs have a negative average tropopause relative height.

The average OT reached an average potential temperature of approximately 381 K and a maximum potential temperature of 388 K. In tropopause relative height this corresponds to 0.76 km and 1.46 km, respectively. In both potential temperature and tropopause relative height, the distributions shift upwards from May through August, before returning downwards through September and October. This is most pronounced in the maximum potential temperature distribution, with the greatest number of OTs falling in the 386 K bin in May, rising to 389 K in August, before falling to 382 K in October. As this trend is present in tropopause relative height as well as potential temperature, it is indicative of more vigorous convection rather than simply being a consequence of the seasonal vertical motion of the tropopause.

Both distributions exhibit long tails. This is seen in both directions in potential temperature space, with the lower values being most frequent in May. This is likely due to the climatologically lower tropopause earlier in the season. When normalized to the tropopause, however, the tail of the OT vertical distribution is largely in the higher altitudes. This is visible

https://doi.org/10.5194/acp-2022-641
Preprint. Discussion started: 4 October 2022

Atmospheric Chemistry and Physics Discussions

in the large number of OTs within the highest bins (337 and 572 OTs for average and maximum tropopause height, respectively), which capture all OTs that reach a height above 2.95 km above the tropopause. These infrequent, extreme convective events account for approximately 1.5% of all OTs and occur in every month except October. Ultimately, 83.8% of the 40,918 OTs that occurred during the study period reached 380 K, with 9.7% reaching above 400 K, well into the lower stratosphere.

3.2 Cross-tropopause convection source regions

The seasonal distributions of cross-tropopause convection, however, vary from region to region as shown in Figure 2. In this section, we examine the individual distributions of the largest source regions.

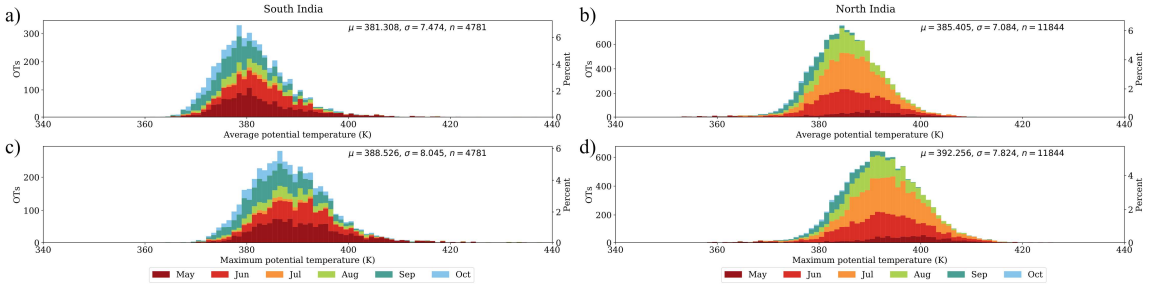

Figure 4 The altitude distribution of OTs within the South India (Figures 4a and 4c) and North India (Figures 4b and 4d) regions. Figures 4a and 4c show the distributions of the average and maximum potential temperature of OTs occurring within the South India region binned by 1 K, respectively. Figures 4b and 4d show the distributions of the average and maximum potential temperature of OTs occurring within the North India region binned by 1 K, respectively. Within each bin, color indicates the fractional contribution of each month, as in Figure 3. The mean, standard deviation, and number of OTs for each distribution is indicated in the upper-right corner.

Figure 4 shows the frequency distributions for both the average and maximum potential temperature of OTs over the South India region (Figures 4a and 4c) and over the North India region (Figures 4b and 4d). Cross-tropopause convection in the North India region is more numerous (11,844 OTs compared to 4,781 OTs), and reaches higher potential temperatures (392 K average maximum potential temperature compared to 389 K) than that over South India. This difference in altitude distribution, however, is primarily due to the latitude dependence of tropopause height. In tropopause relative height, the average maximum heights are 1.46 km and 1.48 km for the North India region and South India region respectively.

The seasonality of the two regions also reveals a key difference. The South India region has the most cross-tropopause convection occurring in May (1380 OTs), June (1011 OTs), and September (1127 OTs), with few OTs appearing in July (152 OTs) and August (521 OTs). In contrast, over North India the majority of cross-tropopause convection occurs in July (4269 OTs), followed by June (3215 OTs) and August (2321 OTs), with relatively little in May (911 OTs) and September (1008 OTs). These two distributions exhibit a northward shift in cross-tropopause convection from May through August across these regions, followed by a southward return into September.

https://doi.org/10.5194/acp-2022-641
Preprint. Discussion started: 4 October 2022

Atmospheric Chemistry and Physics Discussions

This northward migration is consistent with the expected geographic evolution of the Asian monsoon (Kajikawa et al., 2012; Romatschke et al., 2009). Figure 5 shows the monthly geographic distribution of OTs (Figures 5a-5f), average daily OLR (Figures 5g-5l), and average daily precipitation (Figures 5m-5r). In both OLR and precipitation, a similar northward shift is visible in the geographic position of extreme values over land on the subcontinent from May through August, followed by a southward retreat into September and dissipation in October. In addition to the large-scale similarity in latitudinal seasonality, the regions of most frequent cross-tropopause convection are co-located with the most extreme OLR and precipitation values. This agreement among multiple convective indices suggests that the geographic and seasonal trends observed in cross-tropopause convection (OTs) follow the development of the Asian monsoon.

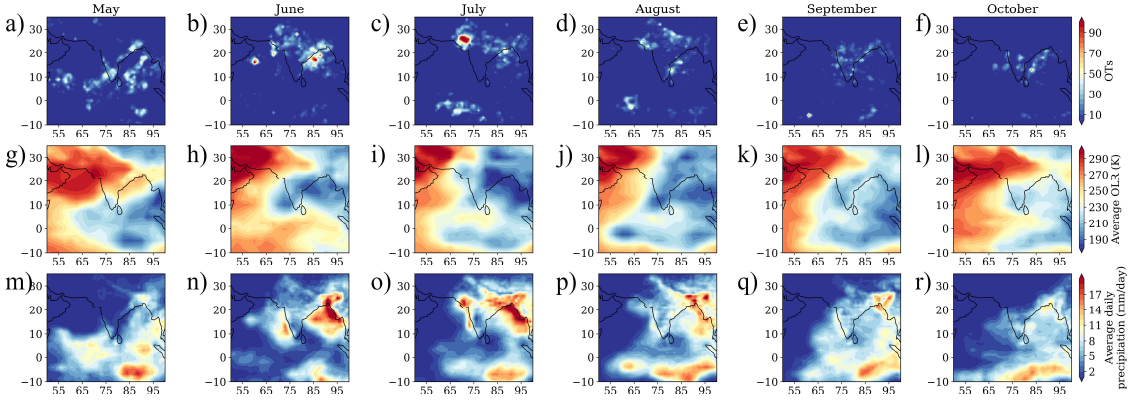

Figure 5 The geographic distribution of monthly convection as shown by OTs (Figures 5a-5f), daily average OLR (Figures 5g-5l), and daily average precipitation (Figures 5m-5r).

Figure 6 shows the frequency distributions for both the average and maximum potential temperature of OTs over the Bay of Bengal region (Figures 6a and 6c) and over the Indian Ocean region (Figures 6b and 6d). Both regions have similar vertical distributions to the total OT distribution (Figure 3) in terms of the average (380 K and 386 K for the Bay of Bengal, and 381 K and 387 K for the Indian Ocean). The most significant contrast between these regions is the differences in the seasonality of cross-tropopause convection.

https://doi.org/10.5194/acp-2022-641
Preprint. Discussion started: 4 October 2022

Atmospheric Chemistry and Physics Discussions

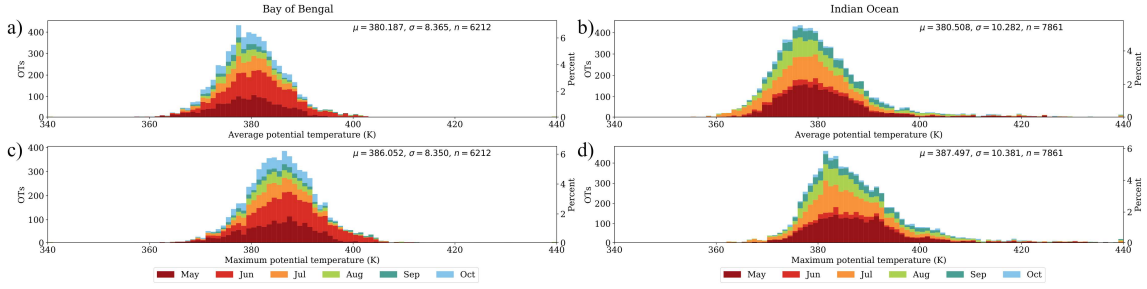

Figure 6 As Figure 4, but for the potential temperature distributions of OTs over the Bay of Bengal region (Figures 6a and 6c) and the Indian Ocean region (Figure 6b and 6d).

The Bay of Bengal has significant OT occurrence across all months, with the most activity occurring earlier in May and June (1574 and 1984 OTs, respectively). As shown in Figure 5, the monthly geographic distribution of the Bay of Bengal OTs matches the spatial distributions of low OLR and high precipitation. However, while the spatial distribution is replicated, the relative importance of each month in terms of number of OTs, is not distinguishable in either OLR or precipitation for the Bay of Bengal region. This is most apparent in the months of July and August (915 and 572 OTs, respectively), which exhibit the greatest extent of areas of low OLR and high precipitation, but have fewer cross-tropopause convective events than May and June. This is likely due to the lower tropopause in the earlier months as shown in Figures 6a and 6c in which the lowermost potential temperature bins have a greater proportion of May and June contributions. Therefore, while convection over the Bay of Bengal may have a maximum in July and August, this convection is less likely to cross the tropopause.

The most notable feature of the distribution of cross-tropopause convection in the Indian Ocean region, is the relative lack of OTs in the month of June (482 OTs, 6.1%), compared to the other summer months with the next least convectively active month, August, having 1379 OTs (17.5%). Figure 5 suggests that this pause in cross-tropopause convection reflects a lack of convection more generally. Both the OLR and precipitation indices show that the Indian Ocean region has much less convective activity in June.

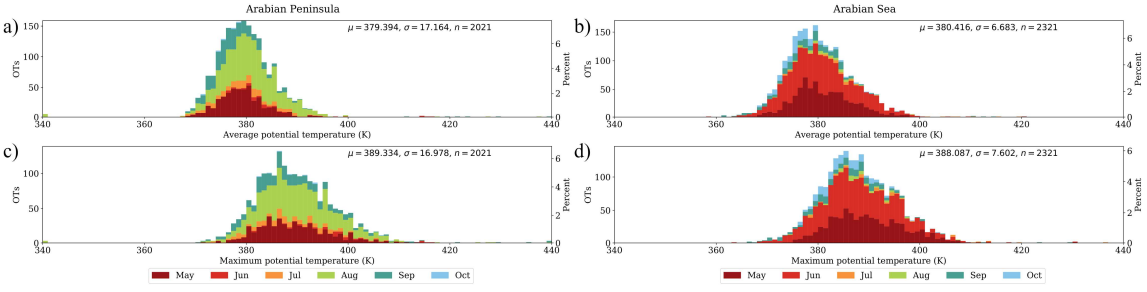

Figure 7 As Figure 4, but for the potential temperature distributions of OTs over the Arabian Peninsula region (Figures 7a and 7c) and the Arabian Sea region (Figure 7b and 7d).

https://doi.org/10.5194/acp-2022-641
Preprint. Discussion started: 4 October 2022

Atmospheric Chemistry and Physics Discussions

Figure 7 shows frequency distributions for both the average and maximum potential temperature of OTs over the Arabian Peninsula region (Figures 7a and 7c) and over the Arabian Sea region (Figures 7b and 7d). Though these regions are minority contributors to cross-tropopause convection over the entire study region (4.9 and 5.7% for the Arabian Peninsula and Arabian Sea regions, respectively), they exhibit high geographic concentrations of OTs comparable to the more convectively active regions. The Arabian Peninsula and Arabian Sea regions have maximum OT densities of 174 and 138 OTs per 1°x1° grid cell, respectively, compared to 154 OTs per 1°x1° grid cell for the North India region. Further, while the vertical distribution of the cross-tropopause convection in these regions is similar to the overall distribution across the entire study region, they have distinct seasonal features.

The cross-tropopause convection in the Arabian Peninsula region occurs almost exclusively in May and August (which together contribute 1459 OTs, 72.2%). June, July and September only contribute 41 (2.0%), 164 (8.1%), and 347 OTs (17.2%) respectively. This cross-tropopause convection also occurs primarily in the southwestern edge of the Arabian Peninsula, along the Red Sea coast. This concentration of OTs is co-located with the Asir Mountains and is likely orographic in origin (Abdullah & Al-Mazroui, 1998; Chakraborty et al., 2006; Segele & Lamb, 2005). Figure 8 shows the monthly geographic distribution of OTs (Figures 8a-8f), average daily OLR (Figures 8g-8l), average daily precipitation (Figures 8m-8r), and average daily specific humidity at 850 hPa (Figures 8s-8x). Although OLR and precipitation show similar local maxima in the same region of the east coast of the Red Sea, they do not reproduce the relative intensity evident in the OTs. The specific humidity at 850 hPa, however, shows more intense local maxima along the Red Sea east coast, further indicating orographic lifting of this moist air as a likely source of cross-tropopause convection in this region.

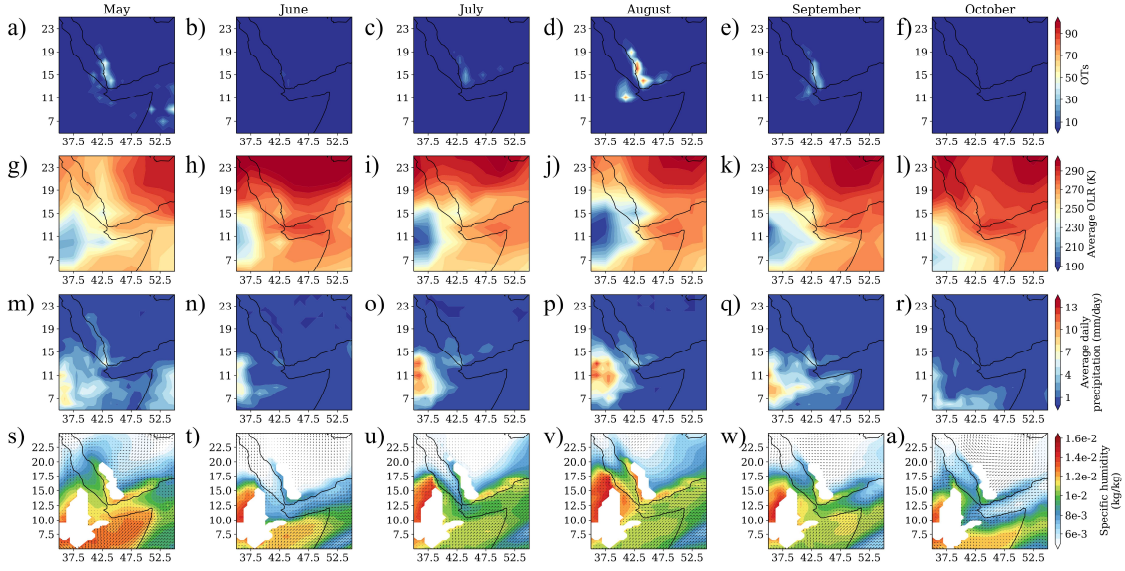

https://doi.org/10.5194/acp-2022-641
Preprint. Discussion started: 4 October 2022


Atmospheric Chemistry and Physics Discussions

Figure 8 The geographic distribution of monthly convection over east Africa and the southwest Arabian Peninsula as shown by OTs (Figures 8a-8f), daily average OLR (Figures 8g-8l), and daily average precipitation (Figures 8m-8r). Additionally, the specific humidity and wind vectors at 850 hPa from MERRA-2 are shown (Figure 8s-8x).

The OT distribution over the Red Sea region is in part decoupled from larger scale patterns evident in OLR and precipitation. The different distributions agree in that the most convectively intense month according to the OLR and precipitation distribution occurs in August, which also has the most OTs over Ethiopia, and there is some agreement in the location of maxima over the Arabian Peninsula. However, both OLR and precipitation indicate more intense convection is occurring over Ethiopia than over the Red Sea coast, and that there is substantial convection during June and July, when there is little evidence for cross-tropopause convection in the OTs. This indicates that the southeast coast of the Red Sea may be uniquely conducive to cross-tropopause convection, possibly because of the potential orographic initiation. As the study region does not extend further into Africa and the study period is limited to 2017, however, this conclusion is preliminary. For context, the global studies of extreme convection also indicate more convective activity over the Arabian Peninsula than over Ethiopia (Liu & Lie, 2016; Liu et al., 2020). Further research into the circumstances that result in this tight geographic concentration is warranted.

The Arabian Sea region has most of its cross-tropopause convection confined to the two months of May and June as seen in Figures 7b and 7d. During August-October combined, only 404 OTs (17.4%) occur. This seasonal dependence is largely reflective of convective trends in this region. As before, Figure 5 shows the monthly geographic distribution of OTs (Figures 5a-5f), average daily OLR (Figures 5g-5l), and average daily precipitation (Figures 5m-5r) of this region. Precipitation in particular, has maxima co-located with the regions of most OT activity during May and June. OLR has similar overall geographic distributions, but weaker. For example, the "point" maxima in June is present in the OLR distribution, but is not as intense relative to the overall region. The location of the June cross-tropopause convection is geographically concentrated to such an extent because it is likely sourced from a single large storm system that passed through the Arabian Sea during the first week of June, which is in its tropical cyclone season at this time (Deshpande et al., 2021; Evan et al., 2011). We note that this geographic "point" source of convective influence over the Arabian Sea is also visible in a trajectory study, Legras & Bucci (2020), of the 2017 summer season of the Asian monsoon that initiates forward trajectories at satellite based cloud top observations (as compared to the OTs examined here).

4 Conclusions

We construct a database of cross-tropopause convection in the Asian monsoon region for the months of May through October of 2017 using Meteosat-8 geostationary satellite detections of OTs. We analyze the geographic, seasonal and vertical distribution of the 40,918 OTs to identify regions of high frequency and high density cross-tropopause convection and their particular seasonal trends and characteristics. Additionally, through comparison with OLR and precipitation observations we place the cross-tropopause database in the context of tropospheric convection generally.

https://doi.org/10.5194/acp-2022-641
Preprint. Discussion started: 4 October 2022


Atmospheric Chemistry and Physics Discussions

We find that cross-tropopause convection is active in the Asian monsoon region during the months of May through August (with daily averages of these months above 300 OTs/day) and declines through September and October. Most of this convection occurs within the Indian subcontinent with North India contributing 29.0% of all OTs, South India contributing 11.7% of all OTs, and the Bay of Bengal contributing 15.2% of all OTs. Together with the Indian Ocean region (19.2%), the most cross-tropopause convection occurs in these regions, and they cumulatively account for 75.1% of all OTs. While the Arabian Peninsula and Arabian Sea regions are smaller sources of cross-tropopause convection (4.9% and 5.7%, respectively), they exhibit geographic OT densities comparable to the major source regions. The majority of cross-tropopause convection within the entire study region reaches a maximum height above 380 K (83.8%), with an average OT maximum height of 387 K corresponding to 1.46 km above the tropopause.

We further identify distinct, differing seasonal trends within these subregions. Within the four most active regions (North India, Indian Ocean, Bay of Bengal, and South India) the geographic and seasonal distribution of cross-tropopause convection matches the distribution of general tropospheric convection as observed in OLR and precipitation. For the North India, South India, and Bay of Bengal regions this results in the distribution of OTs following the development of the Asian Monsoon, with its north-south movement across the study period. Within the Arabian Peninsula and Arabian Sea regions, the seasonal and geographic distributions are tightly confined to the conditions defined by the unique sources of cross-tropopause convection of these regions. In the Arabian Peninsula, OTs are primarily observed in May and August, corresponding to a confluence of low-level moisture along the western slope of the Asir Mountains indicating a likely orographic source of convection. In the Arabian Sea, most OTs occur in June, with a "hotspot" corresponding to a single large storm system. Whether these trends in cross-tropopause convection are recurring features should be explored in future research.

Our examination of cross-tropopause convection that directly impacts the lower stratosphere is complementary to the large body of research that has examined the effects of deep tropospheric convection that subsequently enters the lower stratosphere through diabatic ascent. In contrast to prior work that has emphasized either oceanic (e.g. James et al., 2008) or land-based (e.g. Bergman et al., 2013) convective source regions as dominant, we find that both contribute significant amounts, though with different seasonal distributions. Further, the land-based cross-tropopause convection centers on North India, not the Tibetan Plateau. This is a significant difference because the Tibetan Plateau is found by some studies to be the primary conduit by which tropospheric convection reaches the lower stratosphere (Bergman et al., 2013; Pan et al., 2016). These differences in the distributions of cross-tropopause convection, and deep convection more generally, most agree with the studies that conclude that the Tibetan Plateau is a region favorable to diabatic ascent but not itself a major convective source (Legras & Bucci, 2020; Tissier & Legras., 2016). From this perspective, it is not expected for the Tibetan Plateau to be a large contributor of cross-tropopause convection.

As this analysis only covers May through October of 2017, it is unable to assess any interannual variability that may alter the seasonal and geographic trends identified here. Furthermore, the geographic boundaries of the OT dataset from the Meteosat coverage do not include two areas that merit further investigation. First, is the convective "hotspot" in the western

https://doi.org/10.5194/acp-2022-641
Preprint. Discussion started: 4 October 2022


Atmospheric Chemistry and Physics Discussions

Pacific Ocean, at approximately 135° E, that has been identified as a potential key region for convective influence on the UTLS (e.g. Chen et al., 2012). Second, along the west boundary of our study region, there is indication of additional cross-tropopause convective over Africa, and in particular the African Monsoon region may be an area of significant OT activity. Expanding this research to analyze additional years would allow for an assessment of interannual variability and improve the identification of region specific trends. Further, additional work to normalize geostationary satellite observations would begin the process to assess the global impact of cross-tropopause convection.

Overall, this analysis demonstrates the importance of cross-tropopause convection when considering the influence of convection on the lower stratosphere within the Asian Monsoon region. Not only does the time-scale of the transport mechanism differ from the diabatic ascent pathway, resulting in potentially different chemical species reaching the lower stratosphere, the geographic distribution of cross-tropopause convection indicates a need to account for regions of convective activity beyond those previously identified as primary sources of convective influence via diabatic ascent (e.g. northwest India in Figure 1). Moreover, our work demonstrates that it is critical to consider the longer time-scales given the large seasonal differences in the contributions of each source region. Confining an analysis to a single month would over-emphasize certain source regions while missing others. Given the importance of timing and location when assessing the potential transport of pollution into the lower stratosphere in the Asian Monsoon region, in addition to its importance in determining subsequent transport pathways into the global stratosphere, a broader perspective on convective impacts on the lower stratosphere that includes cross-tropopause convection is critical.

Acknowledgements

We would like to thank the members of the Anderson group for their support. This work has been supported by the National Aeronautics and Space Administration (NASA) under NASA award NNX15AF60G (UV Absorption Cross Sections and Equilibrium Constant of ClOOCl Determined from New Laboratory Spectroscopy Studies of 18 ClOOCl and ClO) and a grant from the National Science Foundation (NSF) Arctic Observing Network (AON) Program under NSF award 1203583 (Collaborative Research: Multi-Regional Scale Aircraft Observations of Methane and Carbon Dioxide Isotopic Fluxes in the Arctic).

Competing Interests

The authors declare that they have no competing interests.

https://doi.org/10.5194/acp-2022-641
Preprint. Discussion started: 4 October 2022

Atmospheric Chemistry and Physics Discussions

Author Contributions

CEC designed the study and performed the analysis. KMB developed the OT detection algorithm and applied it to the Asian monsoon region. JBS provided scientific analysis and assisted with figure development. JGA supervised the study. CEC wrote the manuscript; all co-authors edited and revised the manuscript.

Data availability

Meteosat-8 multispectral imagery: https://navigator.eumetsat.int/start
MERRA-2 reanalysis data: https://disc.gsfc.nasa.gov/
NOAA OLR data: https://psl.noaa.gov/data/gridded/data.olrcdr.interp.html
GPCP Climate Data Record v. 1.3: https://rda.ucar.edu/datasets/ds728.7/

References

Abdullah, M. A. and Al-Mazroui, M. A.: Climatological study of the southwestern region of Saudi Arabia. I. Rainfall analysis, Clim. Res., 9, 213-223, 1998.

Baker, A. K., Schuck, T. J., Slemr, F., van Velthoven, P., Zahn, A., and Brenninkmeijer, C. A. M.: Characterization of non-methane hydrocarbons in Asian summer monsoon outflow observed by the CARIBIC aircraft, Atmos. Chem. Phys., 11, 503-518, 2011.

Bedka, K. M., and Khlopenkov, K.: A probabilistic multispectral pattern recognition method for detection of overshooting cloud tops using passive satellite imager observations, J. Appl. Meteorol. Clim., 55, 1983-2005, 2016.

Bergman, J. W., Fierli, F., Jensen, E. J., Honomichl, S., and Pan, L. L.: Boundary layer sources for the Asian anticyclone: Regional contributions to a vertical conduit, J. Geophys. Res.-Atmos., 118, 2560-2575, 2013.

Brioude, J., Portmann, R. W., Daniel, J. S., Cooper, O. R., Frost, G. J., Rosenlof, K. H., Granier, C., Ravishankara, A. R., Montzka, S. A., and Stohl, A.: Variations in ozone depletion potentials of very short-lived substances with season and emission region, Geophys. Res. Lett., 37, L19804, 2010.

Bucci, S., Legras, B., Sellitto, P., D'Amato, F., Viciani, S., Montori, A., Chiarugi, A., Ravegnani, F., Ulanovsky, A., Cairo, F., and Stroh, F.: Deep-convective influence on the upper troposphere-lower stratosphere composition in the Asian monsoon anticyclone region: 2017 StratoClim campaign results, Atmos. Chem. Phys., 20, 12193-12210, 2020.

Chakraborty, A., Behera, S. K., Mujumdar, M., Ohba, R., and Yamagata, T.: Diagnosis of tropospheric moisture over Saudi Arabia and influences of IOD and ENSO, Mon. Weather Rev., 134, 598-617, 2006.

Chen, B., Xu, X. D., Yang, S., and Zhao, T. L.: Climatological perspectives of air transport from atmospheric boundary layer to tropopause layer over Asian monsoon regions during boreal summer inferred from Lagrangian approach, Atmos. Chem. Phys., 12, 5827-5839, 2012.

https://doi.org/10.5194/acp-2022-641
Preprint. Discussion started: 4 October 2022

475 Clapp, C. E., Smith, J. B., Bedka, K. M., and Anderson, J. G.: Identifying source regions and the distribution of cross-tropopause convective outflow over North America during the warm season, J. Geophys. Res.-Atmos., 124, 13750-13762, 2019.

Clapp, C. E., Smith, J. B., Bedka, K. M., and Anderson, J. G.: Identifying outflow regions of North American monsoon anticyclone-mediated meridional transport of convectively influenced air masses in the lower stratosphere, J. Geophys. Res.-
480 Atmos., 126, e2021JD034644, 2021.

Claxton, T., Hossaini, R., Wild, O., Chipperfield, M. P., and Wilson, C.: On the regional and seasonal ozone depletion potential of chlorinated very short-lived substances, Geophys. Res. Lett., 46, 5489-5498, 2019.

Deshpande, M., Singh, V. K., Gandhi, M. K., Roxy, M. K., Emmanuel, R., and Kumar, U.: Changing status of tropical cyclones over the north Indian Ocean, Clim. Dynam., 57, 3545-3567, 2021.

485 Devasthale, A. and Fueglistaler, S.: A climatological perspective of deep convection penetrating the TTL during the Indian summer monsoon from the AVHRR and MODIS instruments, Atmos. Chem. Phys., 10, 4573-4582, 2010.

Evan, A. T., Kossin, J. P., Chung, C., and Ramanathan, V.: Arabian Sea tropical cyclones intensified by emissions of black carbon and other aerosols, Nature, 479, 94-98, 2011.

Fadnavis, S., Roy, C., Chattopadhyay, R., Sioris, C. E., Rap, A., Müller, R., Kumar, K. R., and Krishnan, R.: Transport of
490 trace gases via eddy shedding from the Asian summer monsoon anticyclone and associated impacts on ozone heating rates, Atmos. Chem. Phys., 18, 11493-11506, 2018.

Fiehn, A., Quack, B., Marandino, C. A., and Krüger, K.: Transport variability of very short lived substances from the West Indian Ocean to the stratosphere, J. Geophys. Res.-Atmos., 123, 5720-5738, 2018.

Fu, R., Hu, Y., Wright, J. S., Jiang, J. H., Dickinson, R. E., Chen, M., Filipiak, M., Read, W. G., Waters, J. W., and Wu, D.
495 L.: Short circuit of water vapor and polluted air to the global stratosphere by convective transport over the Tibetan Plateau, P. Natl. Acad. Sci. U. S. A., 103, 5664-5669, 2006.

Garny, H. and Randel, W. J.: Dynamic variability of the Asian monsoon anticyclone observed in potential vorticity and correlations with tracer distributions, J. Geophys. Res.-Atmos., 118, 13421-13433, 2013.

Gelaro, R., McCarty, W., Suárez, M.J., Todling, R., Molod, A., Takacs, L., Randles, C.A., Darmenov, A., Bosilovich, M.G.,
500 Reichle, R., and Wargan, K.: The Modern-Era Retrospective Analysis for Research and Applications, Version 2 (MERRA-2), J. Climate 30, 5419-5454, 2017.

Griffin, S. M., Bedka, K. M., and Velden, C. S.: A method for calculating the height of overshooting convective cloud tops using satellite-based IR imager and CloudSat cloud profiling radar observations, J. Appl. Meteorol. Clim., 55, 479-491, 2016.

Heath, N. K. and Fuelberg, H. E.: Using a WRF simulation to examine regions where convection impacts the Asian summer
505 monsoon anticyclone, Atmos. Chem. Phys., 14, 2055-2070, 2014.

Hossaini, R., Patra, P. K., Leeson, A. A., Krysztofiak, G., Abraham, N. L., Andrews, S. J., Archibald, A. T., Aschmann, J., Atlas, E. L., Belikov, D. A., Bönisch, H., Carpenter, L. J., Dhomse, S., Dorf, M., Engel, A., Feng, W., Fuhlbrügge, S., Griffiths, P. T., Harris, N. R. P., Hommel, R., Keber, T., Krüger, K., Lennartz, S. T., Maksyutov, S., Mantle, H., Mills, G. P.,

https://doi.org/10.5194/acp-2022-641
Preprint. Discussion started: 4 October 2022

Miller, B., Montzka, S. A., Moore, F., Navarro, M. A., Oram, D. E., Pfeilsticker, K., Pyle, J. A., Quack, B., Robinson, A. D., Saikawa, E., Saiz-Lopez, A., Sala, S., Sinnhuber, B.-M., Taguchi, S., Tegtmeier, S., Lidster, R. T., Wilson, C., and Ziska, F.: A multi-model intercomparison of halogenated very short-lived substances (TransCom-VSLS): linking oceanic emissions and tropospheric transport for a reconciled estimate of the stratospheric source gas injection of bromine, Atmos. Chem. Phys., 16, 9163-9187, 2016.

Huffman, G.J., Adler, R.F., Morrissey, M.M., Bolvin, D.T., Curtis, S., Joyce, R., McGavock, B., and Susskind, J.: Global precipitation at one-degree daily resolution from multisatellite observations, J. Hydrometeorol., 2, 36-50, 2001.

James, R., Bonazzola, M., Legras, B., Surbled, K., and Fueglistaler, S.: Water vapor transport and dehydration above convective outflow during Asian monsoon, Geophys. Res. Lett., 35, L20810, 2008.

Johansson, S., Höpfner, M., Kirner, O., Wohltmann, I., Bucci, S., Legras, B., Friedl-Vallon, F., Glatthor, N., Kretschmer, E., Ungermann, J., and Wetzel, G.: Pollution trace gas distributions and their transport in the Asian monsoon upper troposphere and lowermost stratosphere during the StratoClim campaign 2017, Atmos. Chem. Phys., 20, 14695-14715, 2020.

Kajikawa, Y., Yasunari, T., Yoshida, S., and Fujinami, H.: Advanced Asian summer monsoon onset in recent decades, Geophys. Res. Lett., 39, L03803, 2012.

Legras, B. and Bucci, S.: Confinement of air in the Asian monsoon anticyclone and pathways of convective air to the stratosphere during the summer season, Atmos. Chem. Phys., 20, 11045-11064, 2020.

Lelieveld, J., Bourtsoukidis, E., Brühl, C., Fischer, H., Fuchs, H., Harder, H., Hofzumahaus, A., Holland, F., Marno, D., Neumaier, M., Pozzer, A., Schlager, H., Williams, J., Zahn, A., and Ziereis, H.: The South Asian monsoon – pollution pump and purifier, Science, 361, 270-273, 2018.

Liebmann, B. and Smith, C. A.: Description of a complete (interpolated) outgoing longwave radiation dataset, B. Am. Meteorol. Soc., 77, 1275-1277, 1996.

Liu, N. and Liu, C.: Global distribution of deep convection reaching tropopause in 1 year GPM observations, J. Geophys. Res.-Atmos., 121, 3824-3842, 2016.

Liu, N., Liu, C., and Hayden, L.: Climatology and detection of overshooting convection from 4 years of GPM precipitation radar and passive microwave observations, J. Geophys. Res.-Atmos., 125, 2020.

Luo, J., Pan, L. L., Honomichl, S. B., Bergman, J. W., Randel, W. J., Francis, G., Clerbaux, C., George, M., Liu, X., and Tian, W.: Space-time variability in UTLS chemical distribution in the Asian summer monsoon viewed by limb and nadir satellite sensors, Atmos. Chem. Phys., 18, 12511-12530, 2018.

Müller, S., Hoor, P., Bozem, H., Gute, E., Vogel, B., Zahn, A., Bönisch, H., Keber, T., Krämer, M., Rolf, C., Riese, M., Schlager, H., and Engel, A.: Impact of the Asian monsoon on the extratropical lower stratosphere: trace gas observations during TACTS over Europe 2012, Atmos. Chem. Phys., 16, 10573-10589, 2016.

Pan, L. L., Honomichl, S. B., Kinnison, D. E., Abalos, M., Randel, W. J., Bergman, J. W., and Bian, J.: Transport of chemical tracers from the boundary layer to stratosphere associated with the dynamics of the Asian summer monsoon, J. Geophys. Res.-Atmos., 121, 14159-14174, 2016.

https://doi.org/10.5194/acp-2022-641
Preprint. Discussion started: 4 October 2022


Atmospheric Chemistry and Physics Discussions

Park, M., Randel, W. J., Gettelman, A., Massie, S. T., and Jiang, J. H.: Transport above the Asian summer monsoon anticyclone inferred from Aura Microwave Limb Sounder tracers, J. Geophy. Res., 112, D16309, 2007.

Pisso, I., Haynes, P. H., and Law, K. S.: Emission location dependent ozone depletion potentials for very short-lived halogenated species, Atmos. Chem. Phys., 10, 12025-12036, 2010.

Popovic, J. M. and Plumb, R. A.: Eddy shedding from the upper-tropospheric Asian monsoon anticyclone, J. Atmos. Sci., 58, 93-104, 2001.

Randel, W. J., Park, M., Emmons, L., Kinnison, D., Bernath, P., Walker, K. A., Boone, C., and Pumphrey, H.: Asian monsoon transport of pollution to the stratosphere, Science, 238, 611-613, 2010.

Rolf, C., Vogel, B., Hoor, P., Afchine, A., Günther, G., Krämer, M., Müller, R., Müller, S., Spelten, N., and Riese, M.: Water vapor increase in the lower stratosphere of the Northern Hemisphere due to the Asian monsoon anticyclone observed during the TACTS/ESMVal campaigns, Atmos. Chem. Phys., 18, 2973-2983, 2018.

Romatschke, U. and Houze, R. A.: Characteristics of precipitating convective systems in the South Asian monsoon, J. Hydrometeorol., 12, 3-26, 2011.

Santee, M. L., Manney, G. L., Livesey, N. J., Schwartz, M. J., Neu, J. L., and Read, W. G.: A comprehensive overview of the climatological composition of the Asian summer monsoon anticyclone based on 10 years of Aura Microwave Limb Sounder measurements, J. Geophys. Res.-Atmos., 122, 5491-5514, 2017.

Segele, Z. T. and Lamb, P. J.: Characterization and variability of Kiremt rainy season over Ethiopia, Meteorol. Atmos. Phys., 89, 153-180, 2005.

Tegtmeier, S., Atlas, E., Quack, B., Ziska, F., and Krüger, K.: Variability and past long-term changes of brominated very short-lived substances at the tropical tropopause, Atmos. Chem. Phys., 20, 7103-7123, 2020.

Tissier, A.-S. and Legras, B.: Convective sources of trajectories traversing the tropical tropopause layer, Atmos. Chem. Phys., 16, 3383-3398, 2016.

Vernier, J.-P., Fairlie, T. D., Natarajan, M., Wienhold, F. G., Bian, J., Martinsson, B. G., Crumeyrolle, S., Thomason, L. W., and Bedka, K. M.: Increase in upper tropospheric and lower stratospheric aerosol levels and its potential connection with Asian pollution, J. Geophys. Res.-Atmos., 120, 1608-1619, 2015.

Vernier, J.-P., Fairlie, T. D., Ratnam, M. V., Gadhavi, H., Kumar, B. S., Natarajan, M., Pandit, A. K., Raj, S. T. A., Kumar, A. H., Jayaraman, A., Singh, A. K., Rastogi, N., Sinha, P. R., Kumar, S., Tiwari, S., Wegner, T., Baker, N., Vignelles, D., Stenchikov, G., Shevchenko, I., Smith, J., Bedka, K., Kesarkar, A., Singh, V., Bhate, J., Ravikiran, V., Rao, M. D., Ravindrababu, S., Patel, A., Vernier, H., Wienhold, F. G., Liu, H., Knepp, T. N., Thomason, L., Crawford, J., Ziemba, L., Moore, J., Crumeyrolle, S., Williamson, M., Berthet, G., Jégou, F., and Renard, J.-B.: BATAL: The Balloon Measurement Campaigns of the Asian Tropopause Aerosol Layer, B. Am. Meteorol. Soc., 99 (5), 955-973, 2018.

Vogel, B., Günther, G., Grooß, J.-U., Hoor, P., Krämer, M., Müller, S., Zahn, A., and Riese, M.: Fast transport from Southeast Asia boundary layer sources to northern Europe: rapid uplift in typhoons and eastward eddy shedding of the Asian monsoon anticyclone, Atmos. Chem. Phys., 14, 12745-12762 2014.

https://doi.org/10.5194/acp-2022-641
Preprint. Discussion started: 4 October 2022

von Hobe., M., Ploeger, F., Konopka, P., Kloss, C., Ulanowski, A., Yushkov, V., Ravegnani, F., Volk, C. M., Pan, L. L., Honomichl, S. B., Times, S., Kinnison, D. E., Garcia, R. R., and Wright, J. S.: Upward transport into and within the Asian monsoon anticyclone as inferred from StratoClim trace gas observations, Atmos. Chem. Phys., 21, 1267-1285, 2021.

Walker, J. M. and Bordoni, S.: Onset and withdrawal of the large-scale South Asian monsoon: A dynamical definition using change point detection, Geophys. Res. Lett., 43, 11815-11822, 2016.

Wang, B., Wu, R., and Lau, K.-M.: Interannual variability of the Asian summer monsoon: Contrasts between the Indian and Western North Pacific-East Asian monsoons, J. Climate, 14, 4073-4090, 2001.

Wei, W., Zhang, R., Wen, M., Kim, B.-J., and Nam, J.-C.: Interannual variation of the South Asian high and its relation with Indian and East Asian summer monsoon rainfall, J. Climate, 28, 2623-2634, 2015.

Wu, Y., Orbe, C., Tilmes, S., Abalos, M., and Wang, X.: Fast transport pathways into the Northern Hemisphere upper troposphere and lower stratosphere during northern summer, J. Geophys. Res.-Atmos., 125, e2019JD031552, 2020.

Yihui, D. and Chan, J. C. L.: The East Asian summer monsoon: an overview, Meteorol. Atmos. Phys., 89 117-142, 2005.

Yost, C. R., Bedka, K. M., Minnis, P., Nguyen, L., Strapp, J. W., Palikonda, R., Khlopenkov, K., Spangenberg, D., Smith, W. L. Jr., Protat, A., and Delanoe, J.: A prototype method for diagnosing high ice water content probability using satellite imager data, Atmos. Meas. Tech., 11, 1615-1637, 2018.

Zipser, E. J., Cecil, D. J., Liu, C., Nesbitt, S. W., and Yorty, D. P.: Where are the most intense thunderstorms on Earth?, B. Am. Meteorol. Soc., 87, 1057-1071, 2006.